

# MRgRFA: physical model and first order correction of PRFS thermometry corrupted by magnetic susceptibility-mediated cavitation's effects

R. Salomir<sup>1</sup>, M. Viallon<sup>1</sup>, S. Terraz<sup>1</sup>, and C. Becker<sup>1</sup>  
<sup>1</sup>Radiologie, Hôpital Universitaire de Genève, Geneva, Switzerland

## Introduction

MR thermometry based on the proton resonance frequency (PRF) method (1) has gained good acceptance for guiding RF ablation of liver tumors (2). Major artifacts in the PRFS thermometry have recently been reported related to per-operative changes of the tissue bulk susceptibility during RF heating (3). They are originating from gas bubbles formation, known as white cavitations' artifacts in US imaging. We propose here a theoretical description of the effects and a first order correction that confirm the source of the spatially related errors in temperature maps and TD during power application.

## Materials and Methods

MRgRFA imaging was performed on a 1.5T MR system (Espree, Siemens AG, Germany) using 2D GRE-EPI PRFS imaging with orthogonal interleaved slices identical to the setup described in (3). Optical fibers were also position to provide a gold standard measurement of T°. The magnitude of the local electric field between the anode and cathode of the bipolar RF electrode is two fold higher as compared to the rest of the conducting surface of the electrode (see Fig.1.a), leading to a T° increase that is approximately four times higher ( $\Delta T \propto E^2$ ) at that specific location. The intrinsic magnetic susceptibility of a gas bubble is ~zero (mass density~10<sup>3</sup> lower relatively to liquid water (or biological tissue) then the tissue to gas susceptibility contrast is ~9 ppm. Therefore, bubbles that form during heating induce dipole magnetic field disturbance. One ppm variation in the z-component of the local magnetic induction is equivalent to 100°C PRFS thermometry error of opposite sign. The change in the local field is considered to be proportional to the local change in bulk susceptibility.

The spatial density of gas fraction in biological tissue is considered to be described by a Gaussian profile with revolution symmetry around the electrode, and mirror symmetric over the median plane between the anode and cathode (see Fig.1.b). This hypothesis is compatible with the thermal buildup produced during RFA as the result of heat diffusion in tissue from a small thermal source (see Fig1.c).

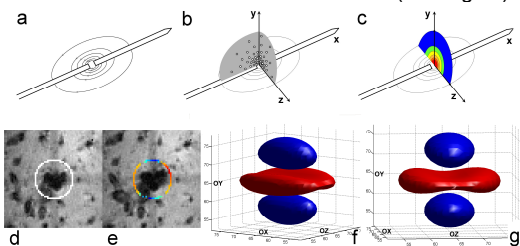


Fig1. Theoretical model for PRFS MR Thermometry errors

**Implementation of Fast Correction:** The principle is to use only MR data. In the imaging plane orthogonal to the electrode and median between the anode and the cathode, we are considering a circular contour centered with the electrode and sized between 1-2 cm diameter, see sagittal GRE-EPI magnitude image in Fig1.d. Given the physical mechanism of heat deposition during RFA procedures, the T° values should be uniform on that ring. For most of the clinical situations addressing liver tumors ablation, the overall heating pattern will fulfill the condition of a circular isotherm in the median plane. The principle of T° correction is to provide on line adjustment of  $\sigma(t)$  in the Eq. [2], so as the corrected T° map  $\Delta T_{corr}$  satisfies the uniformity condition (i.e. isotherm condition) on the circular ring. Equivalent, the cost function to be minimized is the standard deviation of the series of values  $\Delta T_{corr}(\vec{r})$  along the isothermal contour. This principle is insensitive to any spatially uniform phase drift (Bo fluctuation, carrier signal phase etc).

## Results

Fig2. shows that native PRFS-derived T° patterns were significantly changed from theoretical sections from a 3D ellipsoid to asymmetric patterns (axial plane  $\perp$  to the RF electrode and cutting it midway between its anode and cathode active zones, and both a sagittal and coronal plane // to the electrode). Symmetry is recovered after 1<sup>st</sup> order correction. Furthermore, quantitative comparison with gold standard fluoroptic thermometer indicated a residual average error of 4.5°C at the fiber tip location after correction, i.e a factor of 6 of improvement as compared to native PRFS phase subtraction. The residual errors in corrected T° maps were generally higher at the onset time points of the cycles of RFA power application.

Considering the RF electrode positioned parallel to the OX axis (i.e. orthogonal to B<sub>0</sub> direction, according to the frame indicated in Fig1. and also valid inside the MR magnet bore) and the inter anode/cathode gap set at the frame origin, the dynamic source of magnetic susceptibility is approximated in our model as an ellipsoidal object with layers of different susceptibility and attenuating with the distance from the anode/cathode gap:

$$\Delta\chi(\vec{r},t)[ppm] = 9.41 \cdot \exp\left[-\frac{1}{2 \cdot \sigma^2(t)} \cdot \left(\frac{x^2}{\varepsilon^2} + y^2 + z^2\right)\right] \quad [1]$$

where the gas-to-tissue susceptibility contrast was set to the standard value of 9.41 ppm and the specific radius of the bubbles cloud in the sagittal (yOz) plane is denoted as  $\sigma(t)$  [in mm or in pixels]. In the current model, this is the only parameter to be adjusted on line for each dynamic data set. The eccentricity of the ellipsoidal Gaussian source  $\varepsilon$  was estimated by analyzing the shape of the dynamic magnitude artifact in GRE-EPI images with the RF electrode parallel to the B<sub>0</sub> field. The observed effect on the GRE-EPI phase map will depend 1) on the electrode orientation with respect to the magnet frame, and 2) on the imaging plane orientation that is known automatically in DICOM format. According to (4), the effect on the GRE-EPI phase map due to the presence of an additional source of magnetic susceptibility can be calculated based on a fast numerical algorithm, compatible with real time implementation. The master equation used in (4) for correcting the PRFS MR-T° maps has been derived as:

$$\Delta T_{corr}(\vec{r})[^\circ C] = \Delta T_{PRFS}(\vec{r})[^\circ C] + \frac{1}{|\alpha[ppm/^\circ C]|} \cdot FT^{-1}\left[\left(\frac{1}{3} - \frac{k_z^2}{k_x^2 + k_y^2 + k_z^2}\right) \cdot FT[\Delta\chi(\vec{r})[ppm]]\right] \quad [2]$$

where:  $\Delta T_{PRFS}(\vec{r})[^\circ C]$  is the native (i.e. reference subtraction only) PRFS T° map,  $\Delta T_{corr}(\vec{r})[^\circ C]$  is the susceptibility-corrected T° map, the reciprocal-space coordinates are denoted as k<sub>x</sub>, k<sub>y</sub>, k<sub>z</sub> and the source of susceptibility  $\Delta\chi(\vec{r})$  at a given moment of time is expressed according to Eq [1]. The susceptibility-dependent term of Equation [1] is illustrated in Fig1.f and g for the Gaussian model of bubbles. The main magnetic field is considered parallel to the OZ direction as usual. This 3D magnetic perturbation shifts the GRE phase maps concurrently to the T°-dependent PRFS effect. As PRFS coefficient is negative, red lobe corresponds to negative deviation in MR thermometry and blue lobes to positive deviation. Note that Eq.[2] is valid for any dynamic source of susceptibility independently from the hypothesis of Gaussian distribution.

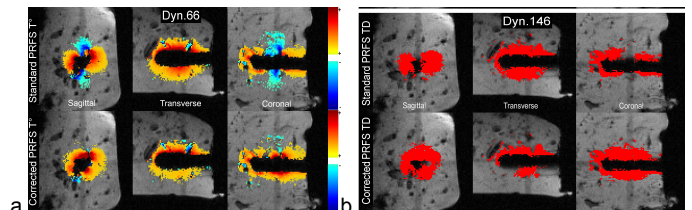


Fig2. Magnitude images with overlaid PRFS T° maps (right) and TD (left) obtained during RF power ON before (first row) and after (second row) dynamic susceptibility correction. A warm/cold color-code ranging from blue (-30°C) to red (50°C and above) show apparent positive/negative T° variations, respectively.

## Conclusion

We have proposed a theoretical description of the effects and demonstrated that a fair agreement between the MR-thermometry and the "gold standard" fluoroptical T° measurement in RF thermo-ablation can be re-established after applying a first order post-processing correction. Our results concern the MR-monitoring of thermal ablation whenever using an active heat source which triggers gas bubbles formation in tissue. Clinical MR-thermometry based on the PRFS method may enable real-time monitoring of RF liver ablation at high field but necessitates a real time correction for the dynamic susceptibility artifacts caused by the heating method itself.

**References:** (1) Ishihara Y. MRM 1995;34(6):814-823. (2) Remp H MRM 2009 (3) Viallon M. prociSMRM 2009. (4) Salomir R. MR (MR Eng) 19B(1), 26-34 (2003)